Implementation of X-Ray Microscopy and Micro-XANES Analysis for Investigations of the Cellular Uptake and Cellular Metabolism of Transition Metals

C. T. Dillon, B. J. Kennedy, P. A. Lay, B. Lai,* Z. Cai,* A. P. J. Stampfl,*[†] P. Ilinski,* D. G. Legnini,* J. Maser,* W. Rodrigues,* G. Shea-McCarthy[‡] and M. Cholewa.[§]

Centre for Heavy Metals Research, School of Chemistry, University of Sydney, NSW, 2006.
*Experimental Facilities Division, Argonne National Laboratory, Argonne, IL, 60439, USA.
[†] Physics Division, Australian Nuclear Science and Technology Organisation, Lucas Heights, NSW, 2234, Australia.
[‡]Brookhaven National Laboratory, Upton, New York.
[§]Gesellschaft fuer Schwerionenforschung mbH, 64 291 Darmstadt, Germany

Corresponding author :   Barry Lai
                           Experimental Facilities Division
                           Argonne National Laboratory
                           Argonne, IL 60439
                           USA
                           Ph.   630-252-6405
                           Fax. 630-252-9303
                           blai@aps.anl.gov

C. T. Dillon, B. J. Kennedy, P. A. Lay, B. Lai, Z. Cai; A. P. J. Stampfl; P. Ilinski, D. G. Legnini, J. Maser, W. Rodrigues, G. Shea-McCarthy and M. Cholewa.

This space should be left blank, except for the names of the authors. (The publisher will re-type the main title, author names and addresses. Please give this information on a separate page.)

Abstract. Micro-SRIXE (synchrotron-radiation-induced X-ray emission) and micro-XAS (X-ray absorption spectroscopy) were used to probe the uptake of exogenous metals by cells. The high flux and the sub-micron resolution of the hard X-ray microprobe, offer the experimenter the ability to obtain highly sensitive spatial and structural information of cellular elements. In this work the uptake of carcinogenic Cr(VI) was compared with that of a relatively non-toxic Cr(III) complex by micro-SRIXE mapping of whole cells. High intracellular Cr concentrations were observed in Cr(VI)-treated cells, while no significant Cr uptake was observed for Cr(III)-treated cells, as is consistent with uptake studies performed by other techniques. Micro-XANES analysis of Cr(V)- and Cr(VI)-treated cells showed that the predominant oxidation product following cellular metabolism was Cr(III). As shown by X-ray microscopic analysis of thin-sectioned cells, however, the reduction of Cr(VI) to Cr(III) did not occur at a fast enough rate to exclude Cr entry into the cell nucleus.

1. INTRODUCTION

It is well documented that Cr(VI) causes cancer following occupational exposure, and it is becoming increasingly evident that adverse effects from Cr(VI) may also extend to environmental exposure [1-3]. Therefore, understanding the mechanisms of Cr carcinogenesis is essential in order to minimise/negate these adverse effects.

X-Ray microscopy (micro-SRIXE) is a powerful technique for spatial analysis of elements at sub-micron to micron resolution. Consequently, the technique has been applied to the study of the cellular uptake of the carcinogen, Cr(VI), the Cr(III) mutagen, $[Cr(phen)_2(OH_2)_2]^{3+}$, and its Cr(V) analogue, $[CrO(phen)_2]^+$. Sub-micron mapping of thin-sectioned cells to determine intracellular targets is also described. Finally, the capabilities of micro-XANES are alluded to in the study of Cr-treated cells wherein information concerning the intracellular metabolism of Cr is deduced.

2. METHOD

All solutions and cell media were prepared in milli-Q water. $Na_2Cr_2O_7$ (Merck, AR grade) was used as received. cis-$[Cr(phen)_2(OH_2)_2](NO_3)_3.2.5H_2O$ was prepared, purified and oxidized to produce the Cr(V) analogue as reported in the literature [4-6].

Whole V79 Chinese hamster lung cells were prepared for X-ray microprobe analysis according to methods detailed by Dillon, *et al.* [6] in which the cells ($\sim 10^6$) were treated with the following Cr complexes: $Na_2Cr_2O_7$, 0.1 mM; cis-$[Cr^{III}(phen)_2(OH_2)_2]^{3+}$ or cis-$[Cr^V(O)_2(phen)_2]^+$, 0.4 mM.

Hard X-ray microprobe experiments were performed on SRI-CAT beamline 2ID-D at the Advanced Photon Source, Argonne National Laboratory [6]. All measurements were conducted using a monochromatic 10-keV X-ray incident beam, and under a He atmosphere in order to eliminate the Ar K-shell fluorescence signal (from air). A number of fluorescence maps (P, Cl, K, Ca, Cr, Fe, Cu, and Zn) corresponding to the integrated K_α fluorescence signal were simultaneously collected for each two-dimensional scan. Whole cells (4-6 per sample) were analyzed using a beam that was focused to approximately 1×0.3 μm^2 using a phase-zone-plate-based scanning hard X-ray microprobe. Scans were acquired in 1-μm steps, and the emitted X-rays were detected for 3 s per point using a Canberra Ultra-LEGe germanium X-ray detector. The detector had an energy resolution of ~ 200 eV over the range of elements examined. Microprobe measurements of thin-sectioned cells were performed using a 0.3-μm

diameter X-ray beam. Areas of (12×12) μm^2 were scanned in steps of 0.3 μm at 6 s per point. The analysis for each set of elemental maps was performed as described [6]. Statistical analyses were performed on the results of whole cell elemental distributions using ANOVA, Tukey-Kramer Multiple Comparison Test [7,8].

Micro-XANES analyses of cellular Cr were performed at Brookhaven National Laboratory, beamline X26A using a 200-μm X-ray beam [9].

3. RESULTS AND DISCUSSION

Micro-SRIXE images of whole cells exposed to Cr(III), Cr(V) or Cr(VI) (Figure 1) showed increased definition in the Cr maps for the Cr(V)- and Cr(VI)-treated cells. The low intensity map of Cr following cell treatment with Cr(III) is consistent with related studies that show that Cr(III) does not enter cells to any appreciable extent, while Cr(VI), which is isostructural with sulfate and phosphate, is readily taken up [2]. Inspection of the Cr maps indicates that Cr is distributed throughout the cell and is not solely located in areas of high P, K, or Zn concentrations.
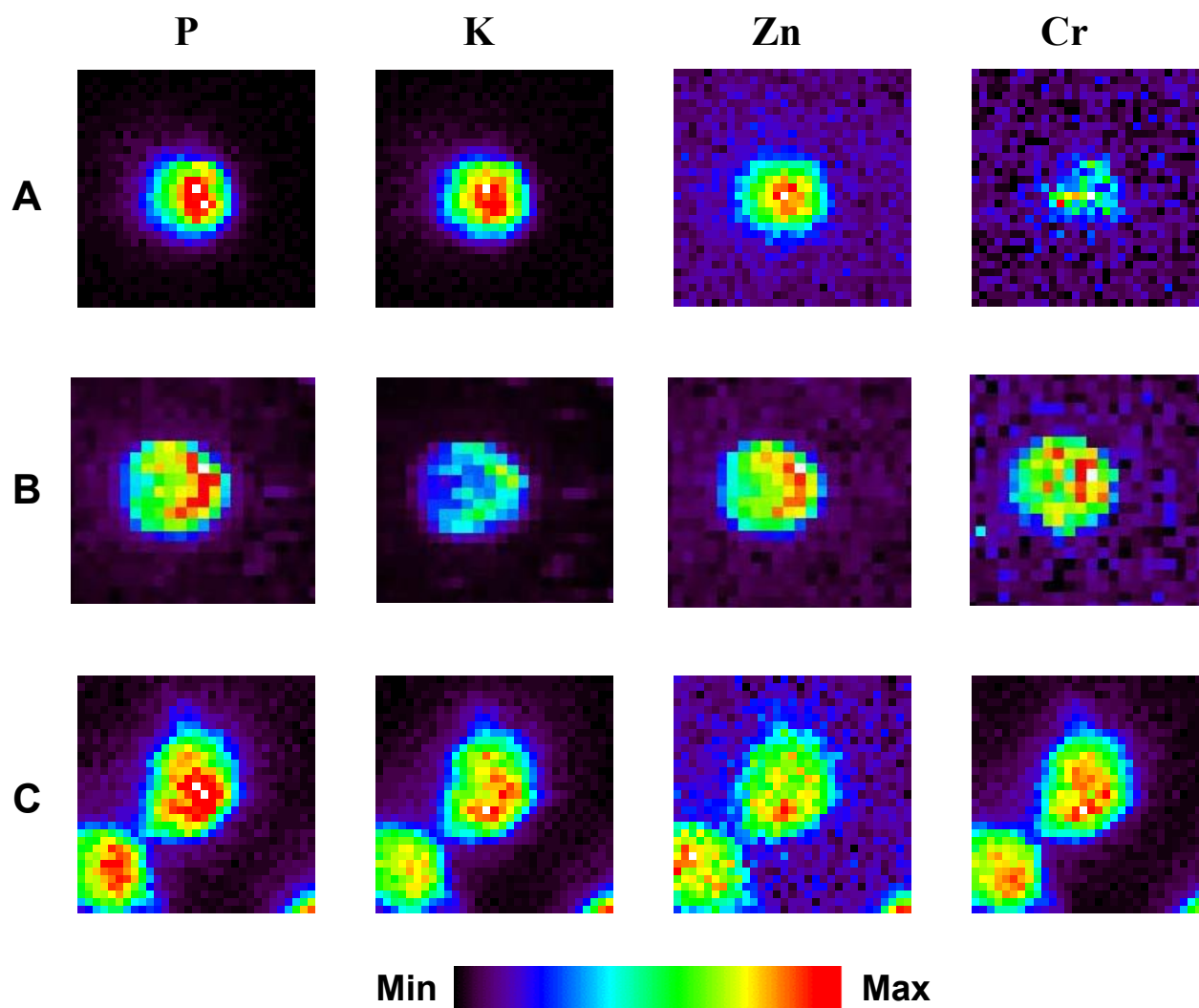

Figure 1. Micro-SRIXE maps of whole V79 Chinese hamster lung cells treated with: A, $[Cr^{III}(phen)_2(OH_2)_2]^{3+}$, 0.4 mM; B, $[Cr^{V}(O)_2(phen)_2]^{+}$, 0.4 mM; and C, $[CrO_4]^{2-}$, 0.1 mM. Adapted with permission from [6], Copyright [2002], Society of Biological Inorganic Chemistry.

Importantly, there was no significant increase in intracellular Cr following treatment with Cr(III) (Figure 2); there were, however, detectable increases in intracellular Cr following treatment with the Cr(V) analogue, $[Cr^{V}(O)_2(phen)_2]^{+}$, and Cr(VI). This is consistent with previous findings that Cr(V) and Cr(VI) increase the incidence of micronuclei formation, an indicator of genotoxic damage (Figure 3). Furthermore, the intracellular oxidation of Cr(III) to Cr(V) may account for the milder but significant increase in micronuclei following treatment with Cr(III) phen.
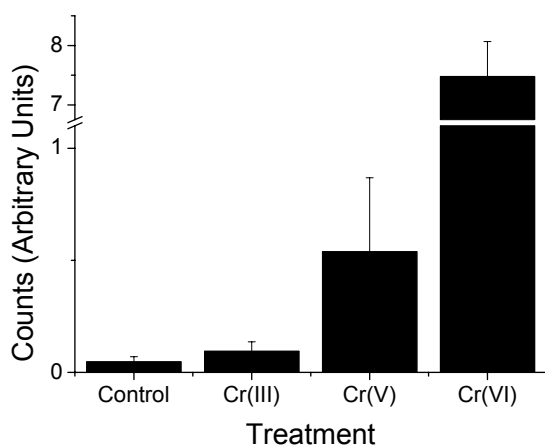
Figure 2. Cellular uptake of Cr following treatment of cells with: $[Cr^{III}(phen)_2(OH_2)_2]^{3+}$, 0.4 mM, $[Cr^{V}(O)_2(phen)_2]^{+}$, 0.4 mM and $[CrO_4]^{2-}$, 0.1 mM. Sample size, **n** = 4-6, and columns represent means ± SD. Reprinted with permission from [6], Copyright [2002], Society of Biological Inorganic Chemistry.
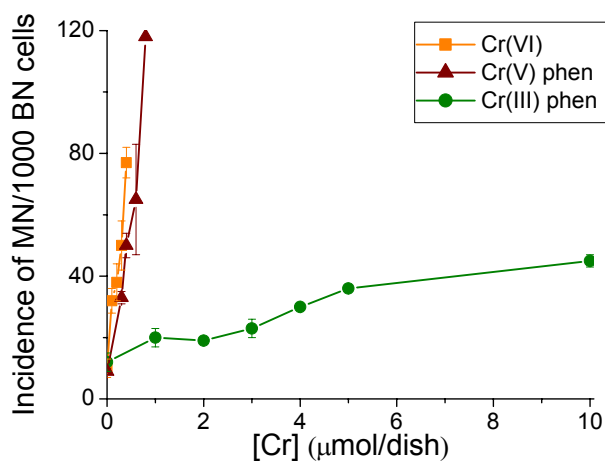
Figure 3. Incidence of micronuclei in binucleated V79 Chinese hamster lung cells following treatment with: $[Cr^{III}(phen)_2(OH_2)_2]^{3+}$, $[Cr^{V}(O)_2(phen)_2]^{+}$ and $[CrO_4]^{2-}$. Sample size, **n** = 2, and data points represent means and error bars represent the SD.

Micro-XAS analyses (Figure 4), performed using a 200-μm diameter beam, were used to establish the oxidation state of the intracellular Cr following exposure to Cr(V) and Cr(VI) mutagens and carcinogens [9]. Most of the Cr was reduced to the impermeable Cr(III) form.
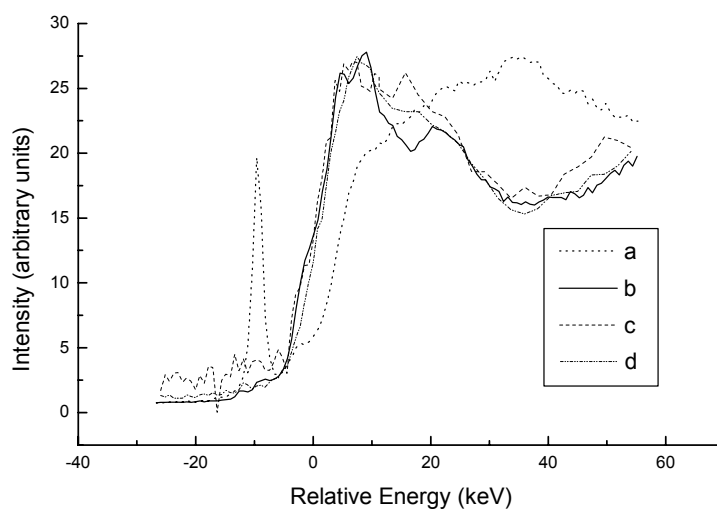
Figure 4. Micro-XANES spectra from the standards: (a) Cr(VI) and (b) Cr(III), and cells treated with (c) Cr(V) and (d) Cr(VI). Reprinted with permission from [9]. Copyright (1997) American Chemical Society.

Micro-SRIXE images of thin-sectioned cells (Figure 5) showed the intracellular Cr distribution following Cr(VI) exposure [6]. Cr was localised in two distinct regions. In one region Cr coexists with high concentrations of Zn (necessary for DNA transcription) and P (a component of the DNA backbone) suggesting that the Cr enters the nucleus. The second region of Cr may have resulted from the rapid reduction of Cr(VI) to Cr(III) and its consequent exclusion from the nucleus. The observation that Cr exists in localised sites, however, suggests encapsulation within a vacuole or some other organelle.
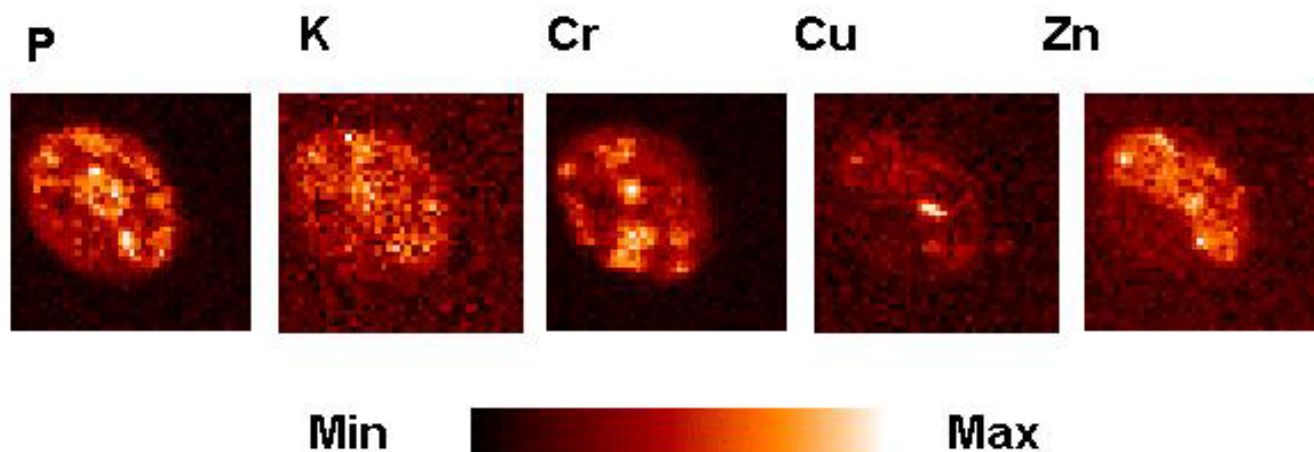
Figure 5. Micro-SRIXE elemental maps of V79 Chinese hamster lung cells that have been treated with Cr(VI). Map dimensions are $12 \times 12 \ \mu m^2$, beam dimensions were $0.3 \ \mu m^2$, step size was $0.3 \ \mu m$. Adapted with permission from [6], Copyright [2002], Society of Biological Inorganic Chemistry.

4. CONCLUSIONS

Clearly, X-ray microscopy can provide crucial information to the understanding of specific biological problems, as shown in this study of Cr carcinogenesis. The ability of the technique to provide direct imaging of elements offers advantages over the imaging of radioactive- or fluorescent-labelled species as it avoids time-consuming, and sometimes hazardous synthetic preparations of the compounds. Similarly, X-ray microscopy avoids artefacts that may arise from altered cell metabolism due to the tagged drug. The ease of selecting scanning fluorescence and micro-XANES modes at the 2ID-D beam-line to within a micron represents a significant advancement towards robust and routine fluorescence and spectroscopic analysis, allowing the uptake of metal-based drugs to be chemically characterised on an intracellular level.

References

[1] IARC (1990) IARC Monographs on the Evaluation of Carcinogenic Risk to Humans: Chromium, Nickel and Welding. Vol. 49. International Agency for Research on Cancer, Lyon, pp. 49-508.
[2] Codd R., Dillon C.T., Levina A. and Lay P.A., *Coord. Chem. Rev.* **216-217**, (2001) 537-582.
[3] Levina A., Codd R., Dillon C.T. and Lay P.A., *Prog. Inorg. Chem.* (2002) Chromium in Biology: Toxicology and Nutritional Aspects. In Press.
[4] Inskeep R.G. and Bjerrum J., *Acta Chem. Scand.* **15**, (1961) 62-68.
[5] Dillon C.T., Lay P.A., Bonin A.M., Dixon N.E. and Sulfab Y., *Aust. J. Chem.* **53** (2000) 411-424.
[6] Dillon C.T., Lay P.A., Kennedy B.J., Stampfl A.P.J., Cai Z., Ilinski P., Rodrigues W., Legnini D.G., Lai B. and Maser J., *J. Biol. Inorg. Chem.* **7** (2002) 640-645.
[7] GraphPad Software, Inc. (1995) GraphPad Prism,. (2.00 edn), San Diego, California.
[8] GraphPad Software, Inc. (1993) GraphPad Instat, San Diego, California.
[9] Dillon C.T., Lay P.A., Cholewa M., Legge G.J.F., Bonin A.M., Collins T.J., Kostka K.L. and Shea-McCarthy G., *Chem. Res. Toxicol.* **10** (1997) 533-535.